Research Article **Open Access**

István Ecsedi* and Ákos József Lengyel

Curved composite beam with interlayer slip loaded by radial load

Abstract: Elastic two-layer curved composite beam with partial shear interaction is considered. It is assumed that each curved layer separately follows the Euler-Bernoulli hypothesis and the load slip relation for the flexible shear connection is a linear relationship. The curved composite beam at one of the end cross sections is fixed and the other end cross section is subjected by a concentrated radial load. Two cases are considered. In the first case the loaded end cross section is closed by a rigid plate and in the second case the radial load is applied immediately to it. The paper gives solutions for radial displacements, slips and stresses. The presented examples can be used as benchmark for the other types of solutions as given in this study.

Keywords: Composite; curved beam; weak shear connection; slip

DOI 10.1515/cls-2015-0004
Received September 23, 2014; accepted November 24, 2014

1 Introduction

Composite members have long been used in many civil engineering structures. In general they consist of two or more elements of the same or different materials connected by some means to form a single structural unit. The problem of layered straight beam with deformable shear connection has been studied for a long time. The first mathematical theories of this type of composite beams were developed by Granholm [1], Pleshkov [2], Stüssi [3], Newmark et al. [4]. The static analysis done by Newmark et al. [4] is based on the Euler-Bernoulli beam theory and become a basis of subsequent investigations of layered beam system with interlayer slip [8, 9, 12]. Today the analytical and numerical solutions and refine of the theory of beams with flexible shear connections are presented by several authors such as Girhammar and Gopu [5], Planic et al. [6], Girhammar and Pan [7], Girhammar [13], Ranzi et al. [14], Schnabl et al. [15], Saje et al. [16]. There exist many other works on this topic, it is not the aim of the present paper to give a complete list on the layered beam with flexible shear connections. Above mentionned papers deal with straight layered beams. There are relatively few works on curved composite beams including the effects of partial shear interactions. For out-of plane loads a numerical method is developed to analyze the time dependent creep and shrinkage behaviour horizontally curved steel-concrete composite beams, including the effects of partial shear interaction by Liu et al. [17]. In paper by Tan and Uy [18] a three-dimensional finite element model is used to simulate composite steel–concrete beams subjected to combined flexure and torsion with the influence of partial shear connection. Tan and Uy gave a detailed description of the torsion induced vertical slip [18]. By Emre and Bradford [19] a total Lagrangian finite element formulation for the elastic analysis of steel–concrete composite beams, that are curved in horizontal plane, has been developed. The presented formulation includes the effects of geometric nonlinearity as well as partial shear interaction in tangential and radial directions [19]. In this paper we consider two-layer curved composite beam with deformable shear connector whose deformation is in-plane deformation. The composite curved beam is subjected to at its one of the end cross section by a radial load as shown in Fig. 1. In the cylindrical coordinate system $Or\varphi z$ the curved layer

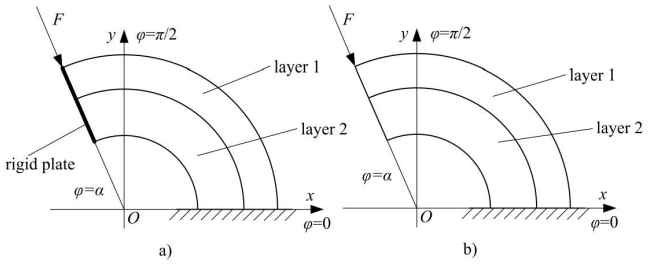

Figure 1: Applied radial load on the end cross section.

***Corresponding Author: István Ecsedi:** Institute of Applied Mechanics, University of Miskolc, Miskolc-Egyetemváros, H-3515 Miskolc, Hungary, Email: mechecs@uni-miskolc.hu
Ákos József Lengyel: Institute of Applied Mechanics, University of Miskolc, Miskolc-Egyetemváros, H-3515 Miskolc, Hungary, Email: mechlen@uni-miskolc.hu

i (i =1,2) occupies the space domain B_i (i =1,2)

$$B_i = \{(r, \varphi, z) \,|\, (r, z) \in A_i, \quad 0 \le \varphi \le \alpha < 2\pi\} \quad (i = 1, 2), \tag{1}$$

where A_i is the cross section of beam component i (i =1,2) (Fig. 2). The common boundary of B_1 and B_2 is denoted by ∂B_{12}

$$\partial B_{12} = \left\{ (r, \varphi, z) \,\middle|\, r = c, \quad 0 \le \varphi \le \alpha, \quad |z| \le \frac{t(c)}{2} \right\}. \tag{2}$$

Here $t = t(r)$ is the thickness of the cross section (Fig. 2). The plane z =0 is the plane of symmetry for the whole two-layer curved beam. The connection between the beam components B_1 and B_2 on their common boundary surface ∂B_{12} in radial direction is perfect, but in circumferential direction may be jump in the displacement field. The possible jump is called the interlayer slip. Two cases of the in-plane deformation are considered. In the first case the end cross section at $\varphi = \alpha$ is closed by a thin rigid plate which is loaded by a given radial load. The bond between the rigid plate and the curved beam is perfect (Fig. 1a). In the second case the radial load F at the cross section $\varphi = \alpha$ is applied immediately as shown in Fig. 1b.

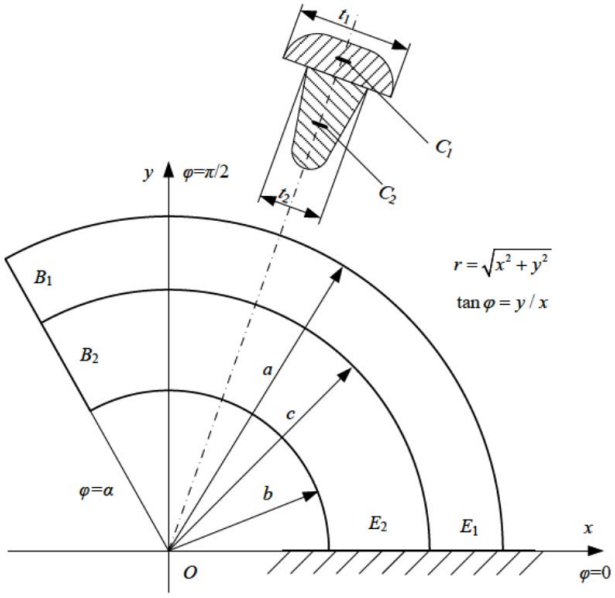

Figure 2: Two-layer curved beam.

2 Governing equations

Denote the unit vectors of cylindrical coordinate system $Or\varphi z$ $\mathbf{e}_r$, $\mathbf{e}_\varphi$, and $\mathbf{e}_z$. We start from the next displacement field to describe the in-plane deformation of the curved composite beam [10]

$$\mathbf{u} = u\mathbf{e}_r + v\mathbf{e}_\varphi + w\mathbf{e}_z, \tag{3}$$

$$u = U(\varphi), \quad w = 0, \quad (r, \varphi, z) \in B = B_1 \cup B_2, \tag{4}$$

$$v(r, \varphi, z) = r\phi_i(\varphi) + \frac{\mathrm{d}U}{\mathrm{d}\varphi}, \qquad (r, \varphi, z) \in B_i \quad (i = 1, 2). \tag{5}$$

Application of the strain-displacement relationships of the linearized theory of elasticity gives [11]

$$\varepsilon_r = \varepsilon_z = \gamma_{r\varphi} = \gamma_{rz} = \gamma_{\varphi z} = 0, \quad (r, \varphi, z) \in B, \tag{6}$$

$$\varepsilon_\varphi = \frac{1}{r}\left(\frac{\mathrm{d}^2 U}{\mathrm{d}\varphi^2} + U\right) + \frac{\mathrm{d}\phi_i}{\mathrm{d}\varphi}, \quad (r, \varphi, z) \in B_i, \quad (i = 1, 2). \tag{7}$$

The strains given by Eqs. 6 and 7 satisfy the requirements of the Euler-Bernoulli beam theory, only the one normal strain component ε_φ is different from zero and all the shearing strains vanish. From the definition of the interlayer slip $s = s(\varphi)$ it follows that (Fig. 2)

$$s(\varphi) = c\left(\phi_1(\varphi) - \phi_2(\varphi)\right). \tag{8}$$

Denote $\tilde{T} = \tilde{T}(\varphi)$ the interlayer shear force acting on unit area of the common boundary surface of B_1 and B_2, which is $ct_2\mathrm{d}\varphi$, since $t_1 > t_2$ (Fig. 2). The value of the interlayer shear force on this surface element is

$$T(\varphi)\mathrm{d}\varphi = \tilde{T}(\varphi)ct_2\mathrm{d}\varphi = kc^2t_2\left(\phi_1(\varphi) - \phi_2(\varphi)\right)\mathrm{d}\varphi, \tag{9}$$

that is

$$T(\varphi) = kc^2t_2\left(\phi_1(\varphi) - \phi_2(\varphi)\right). \tag{10}$$

Here, we assume that

$$\tilde{T}(\varphi) = ks(\varphi) \tag{11}$$

and we note, the unit of slip modulus k is force/(length)^3. According to paper [10] we define the stress resultants normal force and shearing force, and stress couple resultant as

$$N_i = \int_{A_i} \sigma_\varphi \mathrm{d}A, \quad S_i = \int_{A_i} \tau_{r\varphi}\mathrm{d}A, \quad M_i = \int_{A_i} r\sigma_\varphi \mathrm{d}A \quad (i = 1, 2). \tag{12}$$

In Eqs. 12, σ_φ is the normal stress and $\tau_{r\varphi}$ denotes the shearing stress. The virtual work $\tilde{L}$ of the section forces and moment on a kinematically admissible displacement field

$$\tilde{u} = \tilde{U}(\varphi), \quad \tilde{w} = 0, \quad \tilde{v} = r\tilde{\phi}_i + \frac{d\tilde{U}}{d\varphi} \quad (i = 1, 2) \tag{13}$$

can be computed as

$$\tilde{L} = \int\limits_A \sigma_\varphi \tilde{v} \mathrm{d}A + \int\limits_A \tau_{r\varphi} \tilde{u} \mathrm{d}A = M_1 \tilde{\phi}_1 + M_2 \tilde{\phi}_2 + \\ + N \frac{\mathrm{d}\tilde{U}}{\mathrm{d}\varphi} + S\tilde{U}, \quad N = N_1 + N_2, \quad S = S_1 + S_2. \tag{14}$$

From Eq. 14 we obtain the possible combinations of the boundary conditions at the end cross sections

$$S = S_1 + S_2 \text{ or U may be prescribed,} \tag{15}$$

$$N = N_1 + N_2 \text{ or } \frac{\mathrm{dU}}{\mathrm{d}\varphi} \text{ may be prescribed,} \tag{16}$$

$$M_1 \text{ or } \phi_1 \text{ may be prescribed,} \tag{17}$$

$$M_2 \text{ or } \phi_2 \text{ may be prescribed.} \tag{18}$$

The boundary conditions derived above reformulated by introduction the slip function according to the next equation

$$\tilde{\phi}_1 = \frac{\tilde{\mathrm{s}}}{c} + \tilde{\phi}_2. \tag{19}$$

We have from Eqs. 14 and 19

$$\tilde{L} = N \frac{\mathrm{d}\tilde{U}}{\mathrm{d}\varphi} + S\tilde{U} + M_1 \frac{\tilde{\mathrm{s}}}{c} + M\tilde{\phi}_2, \quad M = M_1 + M_2, \tag{20}$$

and the boundary conditions 17 and 18 can be replaced by the next boundary conditions

$$M_1 \text{ or } \frac{\mathrm{s}}{\mathrm{c}} \text{ may be prescribed,} \tag{21}$$

$$M \text{ or } \phi_2 \text{ may be prescribed.} \tag{22}$$

Application of the Hooke's law yields the formula of normal stress σ_φ

$$\sigma_\varphi = E_i \left[\frac{1}{r} \left(\frac{\mathrm{d}^2 U}{\mathrm{d}\varphi^2} + U \right) + \frac{\mathrm{d}\phi_i}{\mathrm{d}\varphi} \right], \quad (r, \varphi, z) \in B_i \\ (i = 1, 2), \tag{23}$$

where E_i is the modulus of elasticity for curved layer i (i =1,2). Combination of Eqs $(12)_{1,2,3}$ with Eq. 23 gives

$$N_i = \frac{A_i E_i}{R_i} W + A_i E_i \frac{\mathrm{d}\phi_i}{\mathrm{d}\varphi}, \quad (i = 1, 2), \tag{24}$$

$$M_i = A_i E_i W + r_i A_i E_i \frac{\mathrm{d}\phi_i}{\mathrm{d}\varphi}, \quad (i = 1, 2). \tag{25}$$

Here

$$\frac{1}{R_i} = \frac{1}{A_i} \int\limits_{A_i} \frac{\mathrm{d}A}{r}, \quad (i = 1, 2), \tag{26}$$

$$r_i = \frac{1}{A_i} \int\limits_{A_i} r \mathrm{d}A, \quad \overline{OC_i} = r_i, \quad (i = 1, 2), \ (Fig.\ 2), \tag{27}$$

and

$$W(\varphi) = \frac{\mathrm{d}^2 U}{\mathrm{d}\varphi^2} + U. \tag{28}$$

The connection between the normal force N and shear force S is as follows [10]

$$S = -\frac{\mathrm{d}N}{\mathrm{d}\varphi}. \tag{29}$$

A simple computation leads to the next results

$$N = \frac{AE_0}{R} W + A_1 E_1 \frac{\mathrm{d}\phi_1}{\mathrm{d}\varphi} + A_2 E_2 \frac{\mathrm{d}\phi_2}{\mathrm{d}\varphi}, \tag{30}$$

$$S = -\left(\frac{AE_0}{R} \frac{\mathrm{d}W}{\mathrm{d}\varphi} + A_1 E_1 \frac{\mathrm{d}^2\phi_1}{\mathrm{d}\varphi^2} + A_2 E_2 \frac{\mathrm{d}^2\phi_2}{\mathrm{d}\varphi^2} \right), \tag{31}$$

$$M = AE_0 W + r_1 A_1 E_1 \frac{\mathrm{d}\phi_1}{\mathrm{d}\varphi} + r_2 A_2 E_2 \frac{\mathrm{d}\phi_2}{\mathrm{d}\varphi}. \tag{32}$$

Here, we introduce A, E_0, R which are defined as

$$E_0 = \frac{E_1 A_1 + E_2 A_2}{A}, \quad A = A_1 + A_2, \tag{33}$$

$$\frac{AE_0}{R} = \frac{A_1 E_1}{R_1} + \frac{A_2 E_2}{R_2}. \tag{34}$$

According to Fig. 1 and Fig. 2, we have

$$S(\varphi) = -F \cos(\varphi - \alpha), \quad 0 \le \varphi \le \alpha, \tag{35}$$

$$N(\varphi) = F \sin(\varphi - \alpha), \quad 0 \le \varphi \le \alpha, \tag{36}$$

$$M(\varphi) = 0, \quad 0 \le \varphi \le \alpha, \tag{37}$$

Let

$$p(\varphi) = \phi_1(\varphi) - \phi_2(\varphi) \tag{38}$$

be. From Eqs. 36, 37 and 38 it follows that

$$AE_0 W + r_1 A_1 E_1 \frac{\mathrm{d}\phi_1}{\mathrm{d}\varphi} + r_2 A_2 E_2 \frac{\mathrm{d}\phi_2}{\mathrm{d}\varphi} = 0, \tag{39}$$

$$AE_0 W + RA_1 E_1 \frac{\mathrm{d}\phi_1}{\mathrm{d}\varphi} + RA_2 E_2 \frac{\mathrm{d}\phi_2}{\mathrm{d}\varphi} = F \sin(\varphi - \alpha), \tag{40}$$

$$\frac{\mathrm{d}\phi_1}{\mathrm{d}\varphi} - \frac{\mathrm{d}\phi_2}{\mathrm{d}\varphi} = \frac{\mathrm{d}p}{\mathrm{d}\varphi}. \tag{41}$$

Eqs. 39- 41 create a system of linear equations for W, $\frac{\mathrm{d}\phi_1}{\mathrm{d}\varphi}$, $\frac{\mathrm{d}\phi_2}{\mathrm{d}\varphi}$, its solution is as follows

$$W(\varphi) = R \frac{\langle AE \rangle_{-1}}{AE_0} \frac{r_1 - r_2}{r_3 - R} \frac{\mathrm{d}p}{\mathrm{d}\varphi} + \frac{r_3 R}{r_3 - R} \frac{F}{AE_0} \sin(\varphi - \alpha), \tag{42}$$

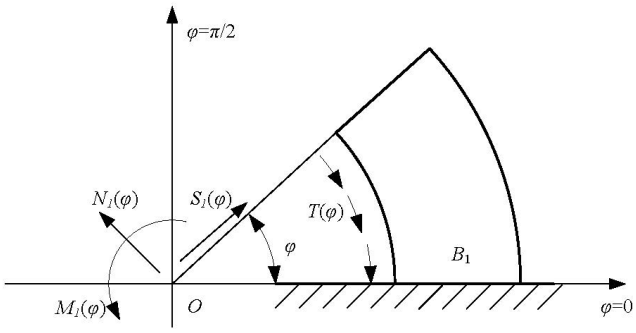

Figure 3: Stress and stress couple resultants and interlayer shear force on beam component 1.

$$\frac{d\phi_1}{d\varphi} = \frac{A_2E_2}{AE_0}\frac{r_2-R}{r_3-R}\frac{dp}{d\varphi} - \frac{R}{r_3-R}\frac{F}{AE_0}\sin(\varphi-\alpha), \quad (43)$$

$$\frac{d\phi_2}{d\varphi} = \frac{A_1E_1}{AE_0}\frac{R-r_1}{r_3-R}\frac{dp}{d\varphi} - \frac{R}{r_3-R}\frac{F}{AE_0}\sin(\varphi-\alpha). \quad (44)$$

Here

$$\langle AE\rangle_{-1} = \frac{A_1E_1A_2E_2}{A_1E_1+A_2E_2}, \quad r_3 = \frac{r_1A_1E_1+r_2A_2E_2}{A_1E_1+A_2E_2}. \quad (45)$$

Moment equilibrium equation for curved beam component 1 can be formulated as (Fig. 3)

$$\frac{dM_1}{d\varphi} + m_1(\varphi) = 0, \quad (46)$$

where the source of $m_1 = m_1(\varphi)$ is the interlayer shear force that is

$$m_1(\varphi) = -cT(\varphi) = -kc^3t_2p(\varphi). \quad (47)$$

Detailed form of Eq. 46 is

$$A_1E_1\frac{dW}{d\varphi} + r_1A_1E_1\frac{d^2\phi_1}{d\varphi^2} - kc^3t_2p(\varphi) = 0. \quad (48)$$

Combination of Eqs. 42, 43 with Eq. 48 gives a second order differential equation for $p = p(\varphi)$

$$\left(A_1E_1R\frac{r_1-r_2}{r_3-R}\frac{\langle AE\rangle_{-1}}{AE_0} + r_1\langle AE\rangle_{-1}\frac{r_2-R}{r_3-R}\right)\frac{d^2p}{d\varphi^2} + \\ -kt_2c^3p = F\frac{A_1E_1}{AE_0}\frac{R}{r_3-R}(r_1-r_3)\cos(\varphi-\alpha). \quad (49)$$

Let

$$\Omega^2 = \frac{kt_2c^3}{A_1E_1R\frac{r_1-r_2}{r_3-R}\frac{\langle AE\rangle_{-1}}{AE_0} + r_1\langle AE\rangle_{-1}\frac{r_2-R}{r_3-R}}, \quad (50)$$

and

$$Q = F\frac{\frac{A_1E_1}{AE_0}R(r_1-r_3)}{A_1E_1\frac{\langle AE\rangle_{-1}}{AE_0}R(r_1-r_2) + \langle AE\rangle_{-1}r_1(r_2-R)} \quad (51)$$

be. By these designations Eq. 52 can be written in the next form

$$\frac{d^2p}{d\varphi^2} - \Omega^2p = Q\cos(\varphi-\alpha). \quad (52)$$

The general solution of differential equation (52) can be represented as

$$p(\varphi) = K_1\sinh\Omega\varphi + K_2\cosh\Omega\varphi - \frac{Q}{1+\Omega^2}\cos(\varphi-\alpha), \quad (53)$$

where K_1 and K_2 are the constants of integration.

The following boundary conditions are used to get the value of K_1 and K_2 when the end cross section at $\varphi = \alpha$ is closed by a rigid plate (Fig. 1a)

$$p(0) = 0, \quad p(\alpha) = 0. \quad (54)$$

A detailed computation for this case leads to the result

$$K_1 = \frac{Q}{1+\Omega^2}\frac{1-\cos\alpha\cosh\Omega\alpha}{\sinh\Omega\alpha}, \quad (55)$$

$$K_2 = \frac{Q}{1+\Omega^2}\cos\alpha. \quad (56)$$

For the second case when there is no rigid plate at the end cross section at $\varphi = \alpha$ (Fig. 1b) we have according to boundary conditions 17 and 18

$$M_1 = A_1E_1\left(W + r_1\frac{d\phi_1}{d\varphi}\right) = 0, \\ M_2 = A_2E_2\left(W + r_2\frac{d\phi_2}{d\varphi}\right) = 0, \quad (57)$$

and we have $N(\alpha) = 0$, that is

$$\frac{AE_0}{R}W + A_1E_1\frac{d\phi_1}{d\varphi} + A_2E_2\frac{d\phi_2}{d\varphi} = 0 \quad \text{if} \quad \varphi = \alpha. \quad (58)$$

From Eqs. 57 and 58 it follows that

$$\frac{d\phi_1}{d\varphi} = 0, \quad \frac{d\phi_2}{d\varphi} = 0 \quad \text{at} \quad \varphi = \alpha, \quad (59)$$

that is

$$\frac{dp}{d\varphi} = 0 \quad \text{at} \quad \varphi = \alpha. \quad (60)$$

The constants of integration in the expression of $p = p(\varphi)$ for the case shown in Fig. 1b are denoted by k_1 and k_2. From Eq. $(54)_1$ and Eq. 60 we get

$$k_1 = -\frac{Q}{1+\Omega^2}\tanh(\Omega\alpha)\cos\alpha, \\ k_2 = \frac{Q}{1+\Omega^2}\cos\alpha. \quad (61)$$

3 Determination of stresses and radial displacement

The circumferential normal stress can be computed by the application of Eq. 23

$$\sigma_\varphi(r,\varphi) = E_i\left(\frac{W}{r} + \frac{d\phi_i}{d\varphi}\right), \\ (r,\varphi,z) \in B_i, \quad (i = 1,2), \quad (62)$$

where W and $\frac{\mathrm{d}\phi_i}{\mathrm{d}\varphi}$, $(i = 1, 2)$ are given by Eqs. 42- 44 and Eq. 53. Assuming that the non-zero stresses are $\sigma_\varphi = \sigma_\varphi(r, \varphi)$, $\tau_{r\varphi} = \tau_{r\varphi}(r, \varphi)$ and $\sigma_r = \sigma_r(r, \varphi)$ we can derive the following equilibrium equations

$$\frac{\partial}{\partial r}\left(rt(r)\sigma_r\right) - t(r)\sigma_\varphi + t(r)\frac{\partial \tau_{r\varphi}}{\partial \varphi} = 0, \tag{63}$$

$$\frac{\partial}{\partial r}\left(rt(r)\tau_{r\varphi}\right) + t(r)\frac{\partial \sigma_\varphi}{\partial \varphi} + t(r)\tau_{r\varphi} = 0. \tag{64}$$

We reformulate Eq. 64 into a new form as

$$\frac{\partial}{\partial r}\left(r^2 t(r)\tau_{r\varphi}\right) + rt(r)\frac{\partial \sigma_\varphi}{\partial \varphi} = 0. \tag{65}$$

Integration of Eq. 65 yields (Fig. 2)

$$\tau_{r\varphi} = -\frac{1}{r^2 t(r)}\int_b^r \rho t(\rho)\frac{\partial \sigma_\varphi}{\partial \varphi}\mathrm{d}\rho, \quad b \le r < c, \tag{66}$$

$$\tau_{r\varphi}(r, \varphi) = \frac{c^2}{r^2}\frac{t_2\tau_2(\varphi)}{t(r)} - \frac{1}{r^2 t(r)}\int_c^r \rho t(\rho)\frac{\partial \sigma_\varphi}{\partial \varphi}\mathrm{d}\rho, \quad c < r \le a, \tag{67}$$

where

$$\tau_2(\varphi) = \lim_{\varepsilon\to 0}\left(\tau_{r\varphi}\left(c - \varepsilon^2, \varphi\right)\right). \tag{68}$$

The validity of formula 67 follows from the next equation

$$t_2\tau_2(\varphi) = t_1 \lim_{\varepsilon\to 0}\left(\tau_{r\varphi}\left(c + \varepsilon^2, \varphi\right)\right). \tag{69}$$

We note that, $\tau_{r\varphi}(c, \varphi)$ can be obtained from the interlayer shear force $T = T(\varphi)$. We consider a surface element on the common boundary of beam component B_1 and B_2 which is $\mathrm{d}a = ct_2\mathrm{d}\varphi$ (Fig. 3). The force acting of this surface element can be expressed in terms of $\tau_{r\varphi}(c, \varphi)$ and $T(\varphi)$. We have

$$T(\varphi)\mathrm{d}\varphi = \tau_{r\varphi}(c, \varphi)ct_2\mathrm{d}\varphi. \tag{70}$$

From Eq. 70 it follows that

$$\tau_{r\varphi}(c, \varphi) = \frac{T(\varphi)}{ct_2} = kc\left[\phi_1(\varphi) - \phi_2(\varphi)\right] \tag{71}$$

according to Eq. 10. The computation of the radial normal stress $\sigma_r = \sigma_r(r, \varphi)$ is based on Eq. 63. From Eq. 63 we obtain

$$\sigma_r(r, \varphi) = \frac{1}{rt(r)}\int_b^r t(\rho)\left(\sigma_\varphi(\rho, \varphi) - \frac{\partial \tau_{r\varphi}}{\partial \varphi}\right)\mathrm{d}\rho, \quad b \le r < c, \tag{72}$$

$$\sigma_r(r, \varphi) = \frac{ct_2\sigma_2(\varphi)}{rt(r)} + \frac{1}{rt(r)}\int_c^r t(\rho)\left(\sigma_\varphi(\rho, \varphi) - \frac{\partial \tau_{r\varphi}}{\partial \varphi}\right)\mathrm{d}\rho, \quad c < r \le a. \tag{73}$$

Here

$$\sigma_2(\varphi) = \lim_{\varepsilon\to 0}\sigma_r\left(c - \varepsilon^2, \varphi\right), \tag{74}$$

and we have used the continuity condition of the radial normal stress resultant which can be formulated as

$$t_2\sigma_2(\varphi) = t_1 \lim_{\varepsilon\to 0}\left(\sigma_r\left(c + \varepsilon^2, \varphi\right)\right). \tag{75}$$

In order to get the expression of radial displacement $U = U(\varphi)$ we use Eqs. 28, 42 and Eq. 53 and boundary conditions at $\varphi = 0$

$$U(0) = 0, \quad \frac{\mathrm{d}U}{\mathrm{d}\varphi} = 0. \tag{76}$$

A detailed computation gives for the first case which is shown in Fig. 1a

$$\begin{aligned} U(\varphi) = &\frac{K_1}{1+\Omega^2}\sinh\Omega\varphi + \frac{K_2}{1+\Omega^2}\cosh\Omega\varphi - \\ &+ \frac{Q}{2\left(1+\Omega^2\right)}\varphi\sin(\varphi - \alpha) - \frac{K_2}{1+\Omega^2}\cos\varphi - \\ &+ \left(K_1\frac{\Omega}{1+\Omega^2} + \frac{Q}{2\left(1+\Omega^2\right)}\sin\alpha\right)\sin\varphi. \end{aligned} \tag{77}$$

Here, we remark that for perfect bond ($k = \infty$)we have according to paper [10]

$$W(\varphi) = \frac{r_3 R}{r_3 - R}\frac{F}{AE_0}\sin(\varphi - \alpha), \tag{78}$$

$$\phi = \phi_1 = \phi_2, \quad \frac{d\phi}{d\varphi} = -\frac{R}{r_3 - R}\frac{F}{AE_0}\sin(\varphi - \alpha), \tag{79}$$

$$\sigma_\varphi(r, \varphi) = E_i\left(\frac{W}{R} + \frac{\mathrm{d}\phi}{\mathrm{d}\varphi}\right), \quad (r, \varphi, z) \in B_i, \quad (i = 1, 2), \tag{80}$$

$$U(\varphi) = \frac{r_3 R}{2\left(r_3 - R\right)}\frac{F}{AE_0}\left[\sin\varphi\cos\alpha - \varphi\cos(\varphi - \alpha)\right]. \tag{81}$$

For the second case (Fig. 1b) the following formula can be derived for $U = U(\varphi)$

$$\begin{aligned} U(\varphi) = &C_1\cosh(\Omega\varphi) + C_2\sinh(\Omega\varphi) + \\ &+ C_3\varphi\cos(\varphi - \alpha) - C_1\cos\varphi - (C_3\cos\alpha + \Omega C_2)\sin\varphi. \end{aligned} \tag{82}$$

In Eq. 82,

$$\begin{aligned} C_1 &= \frac{q\Omega}{1+\Omega^2}k_1, \quad C_2 = \frac{q\Omega}{1+\Omega^2}k_2, \\ C_3 &= -\frac{1}{2}\left(\frac{qQ}{1+\Omega^2} + \frac{r_3 RF}{(r_3 - R)AE_0}\right), \end{aligned} \tag{83}$$

$$q = \frac{R\{IE\}}{AE_0}\frac{r_1 - r_2}{r_3 - R}. \tag{84}$$

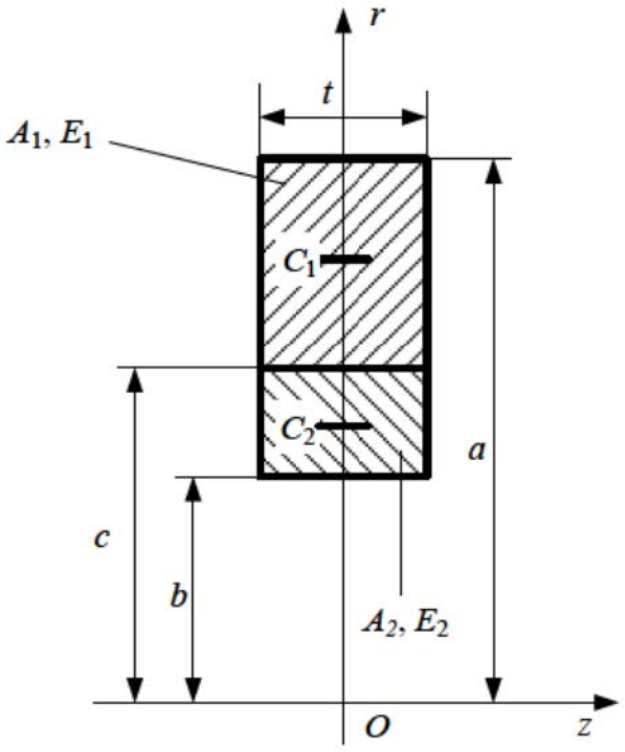

Figure 4: The cross section of the curved composite beam.

4 Examples

The cross section of the two-layer curved beam is shown in Fig. 4. The following data are used:

$$a = 0.04\ [\mathrm{m}], \quad b = 0.02\ [\mathrm{m}], \quad c = 0.03\ [\mathrm{m}],$$
$$t = 0.02\ [\mathrm{m}], \quad E_1 = 10 \times 10^{11}\ [\mathrm{Pa}],$$
$$E_2 = 8 \times 10^{10}\ [\mathrm{Pa}], \quad k = 5 \times 10^{8}\ \left[\frac{\mathrm{N}}{\mathrm{m}^3}\right],$$
$$F = 1000\ [\mathrm{N}], \quad \alpha = \tfrac{3}{4}\pi.$$

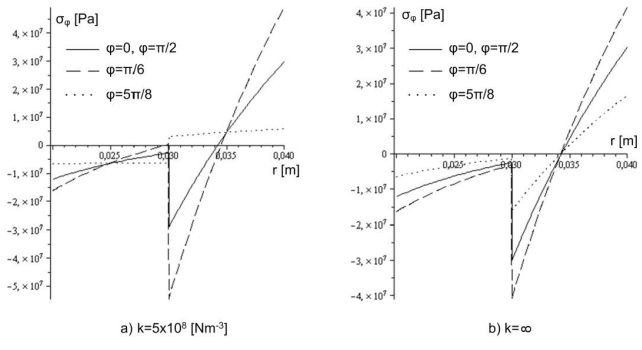

Figure 5: Plots σ_φ for Example 1.

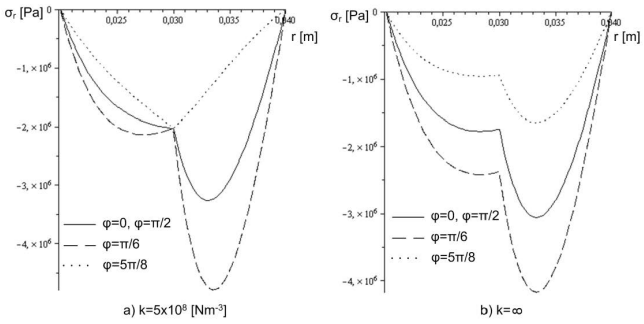

Figure 6: Plots of σ_r for Example 1.

Example 1. End cross section at $\varphi = \alpha$ closed by a rigid plate. The solution of this problem is based on Eqs. 53, 55, 56 and Eq. 77. The graphs of stresses $\sigma_\varphi = \sigma_\varphi(r, \varphi)$, $\sigma_r = \sigma_r(r, \varphi)$, $\tau_{r\varphi} = \tau_{r\varphi}(r, \varphi)$ as a function of radial coordinate r for cross section given by polar angle $\varphi = 0$, $\varphi = \frac{\pi}{6}$, $\varphi = \frac{\pi}{2}$, $\varphi = \frac{5\pi}{8}$ are shown in Figs. 5, 6, 7. The plots of $\tau_{r\varphi}(c, \varphi)$ computed from Eq. 66 and Eq 71 are shown in Fig. 8. The graphs of the radial displacement and slip function as a function of φ are presented in Fig. 9 and Fig. 10. Fig. 11 shows the graphs of bending moment $M_1 = M_1(\varphi)$ and $M_2 = M_2(\varphi)$. The curved beam problem analysed in this paper is a statically determinate problem, that is, in the present case, the bending moment $M = M_1 + M_2$ and shear force S can be computed from the geometry of the curved beam and the applied load. It is evident the equilibrium equations of statics give

$$M(\varphi) = 0, \quad S(\varphi) = -F\cos(\varphi - \alpha). \tag{85}$$

On the other hand we have according to Eq. 32

$$S(\varphi) = -\left(\frac{AE_0}{R}\frac{\mathrm{d}W}{\mathrm{d}\varphi} + A_1E_1\frac{\mathrm{d}^2\phi_1}{\mathrm{d}\varphi^2} + A_2E_2\frac{\mathrm{d}^2\phi_2}{\mathrm{d}\varphi^2}\right). \tag{86}$$

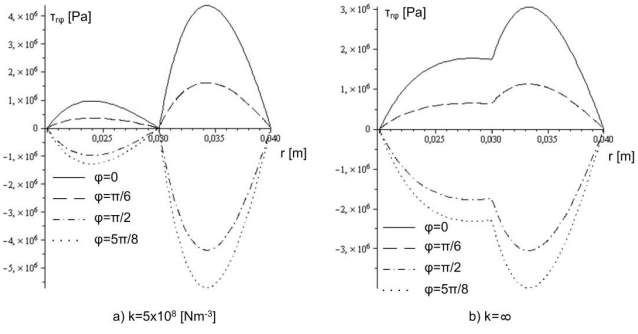

Figure 7: Plots of $\tau_{r\varphi}$ for Example 1.

In this sense Fig. 11 can be considered as a plot of an error indicator which shows that Eq. $(85)_1$ is satisfied. An

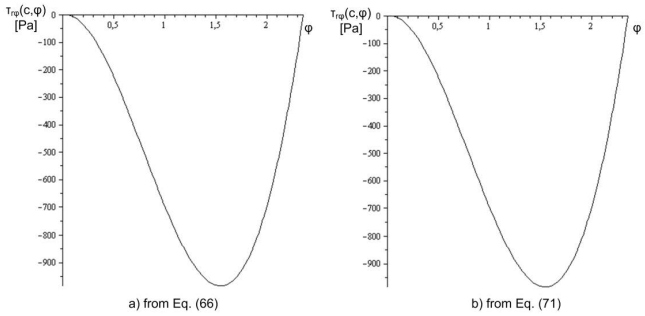

Figure 8: Plots of $\tau_{r\varphi}(c, \varphi)$ for Example 1.

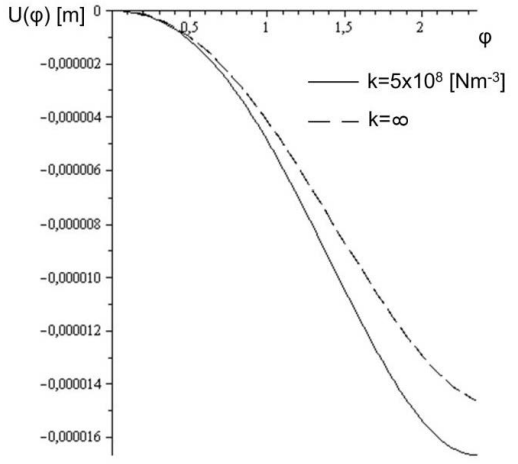

Figure 9: Plots of radial displacement for Example 1.

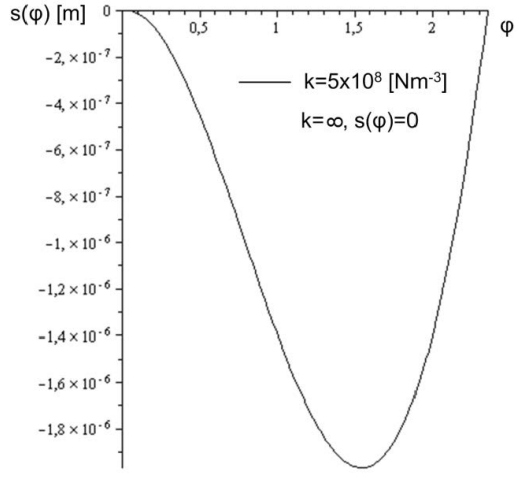

Figure 10: Plots of the slip function for Example 1.

another error indicator is defined by the use of Eqs. $(85)_2$ and 86

$$e(\varphi) = \left| -\left(\frac{AE_0}{R}\frac{\mathrm{d}W}{\mathrm{d}\varphi} + A_1E_1\frac{\mathrm{d}^2\phi_1}{\mathrm{d}\varphi^2} + A_2E_2\frac{\mathrm{d}^2\phi_2}{\mathrm{d}\varphi^2}\right) + F\cos(\varphi-\alpha)\right|. \quad (87)$$

The graph of $e = e(\varphi)$ is shown in Fig. 12.

Example 2. The given radial load applied to the end cross section at $\varphi = \alpha$ immediately as shown in Fig. 1b. The solution of this problem is based on the expression of $p = p(\varphi)$ which is

$$p(\varphi) = k_1\sinh(\Omega\varphi) + k_2\cosh(\Omega\varphi) - \frac{Q}{1+\Omega^2}\cos(\varphi-\alpha) \quad (88)$$

and Eqs. 82, 83. The graphs of stresses $\sigma_\varphi = \sigma_\varphi(r, \varphi)$, $\sigma_r = \sigma_r(r, \varphi)$, $\tau_{r\varphi} = \tau_{r\varphi}(r, \varphi)$ as a function of radial coordinate r for cross section given by polar angle $\varphi = 0$, $\varphi = \frac{\pi}{6}$, $\varphi = \frac{\pi}{2}$, $\varphi = \frac{5\pi}{8}$ are shown in Figs. 13, 14, 15.

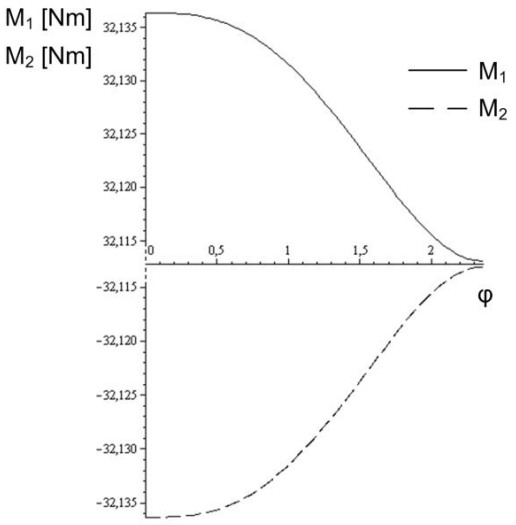

Figure 11: The plots of $M_1 = M_1(\varphi)$ and $M_2 = M_2(\varphi)$ for Example 1.

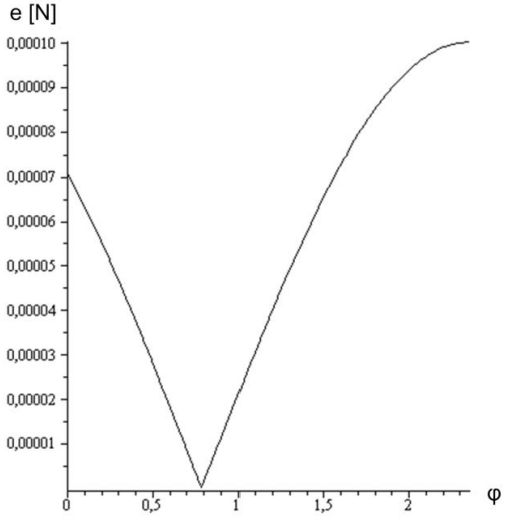

Figure 12: The graph of error indicator $e = e(\varphi)$ for Example 1.

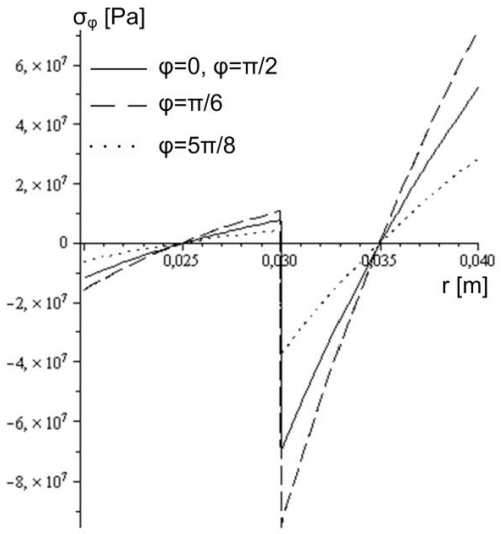

Figure 13: Plots of σ_φ for Example 2.

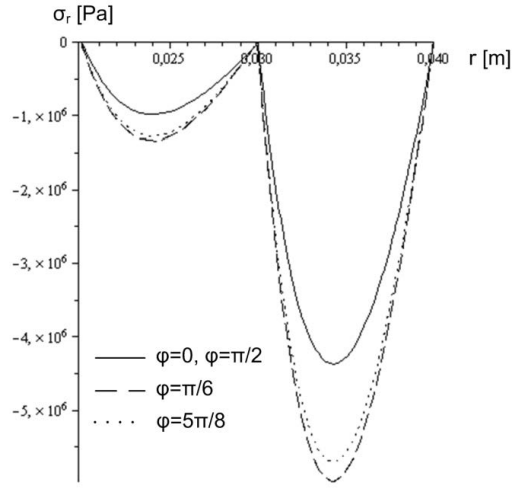

Figure 14: Plots of σ_r for Example 2.

The plots of $\tau_{r\varphi}(c, \varphi)$ computed from Eq. 66 and Eq. 71 are shown in Fig. 16. The graphs of the radial displacement and slip function as a function of φ are presented in Fig. 17 and Fig. 18. Fig. 19 illustrates the plots of $M_1 = M_1(\varphi)$ and $M_2 = M_2(\varphi)$. Obtained numerical results show that the application of rigid plate at the loaded end cross section reduces the radial displacements, slips and normal stresses.

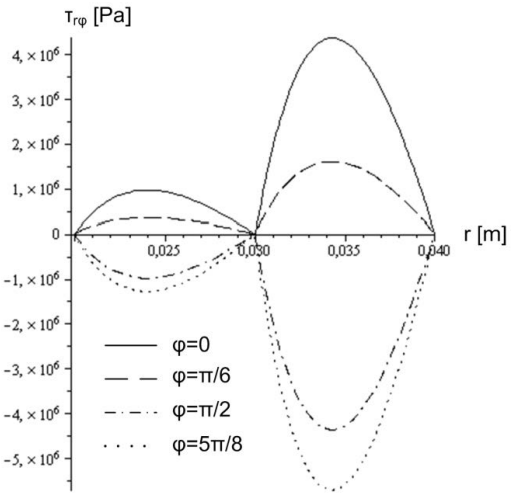

Figure 15: Plots of $\tau_{r\varphi}$ for Example 2.

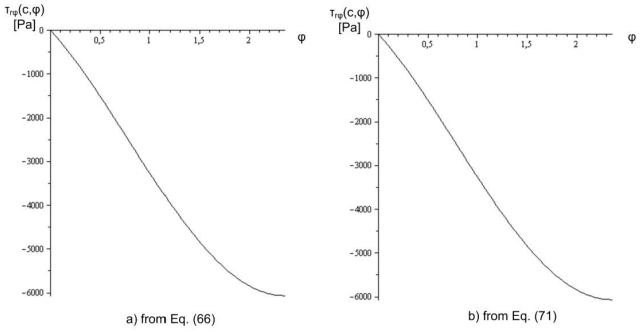

Figure 16: Plots of $\tau_{r\varphi}(c, \varphi)$ for Example 2.

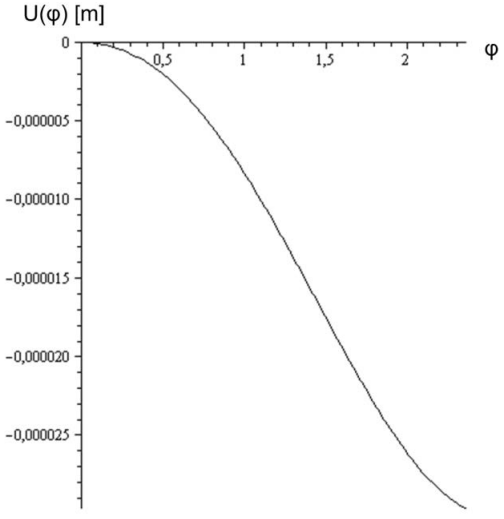

Figure 17: Plots of radial displacement for Example 2.

5 Conclusions

In this paper two-layer curved composite elastic beam with deformable shear connection is analysed. The curved composite beam is loaded at one of the end cross sections by a concentrated radial load. Two cases are considered. In the first case the loaded end cross section is closed by a thin rigid plate. The bond between the rigid plate and the curved beam is perfect. In the second case the radial load

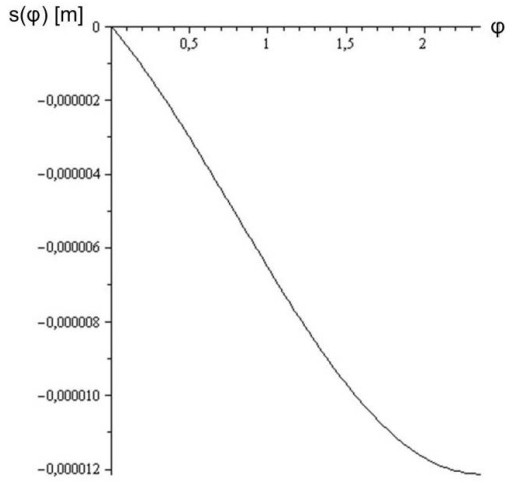

Figure 18: Plots of the slip function for Example 2.

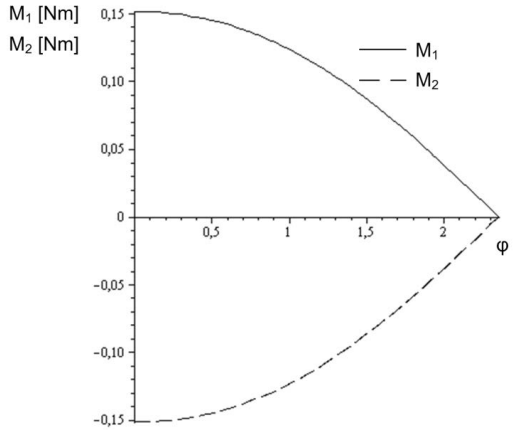

Figure 19: Plots of $M_1(\varphi)$ and $M_2(\varphi)$ for Example 2.

at the loaded end cross section is applied immediately. Paper presents an analytical solution to get the stresses, slips and radial displacements. Numerical examples illustrate the application of developed analytical method. Obtained results can be used as benchmark solution for the approximate solutions of two-layer curved composite beam with interlayer slip.

Acknowledgements: This research was carried out as part of the TÁMOP-4.2.1.B-10/2KONV-2010-0001 project with support by European Union, co-financed by European Social Found.

References

[1] Granholm H., On composite beams and columns with special regard to nailed timber structures, Trans. No. 88. Cholmers University of Technology, Goetborg, Sweden (in Swedish), 1949

[2] Pleskov P.F., Theoretical studies of composite wood structures, Soviet Union (in Russian), 1952

[3] Stüssi F., Zusammengesetzte Vollwandträger (Composed Beams), International Association for Bridge and Structural Engineering (IABSE), 1947, 8, 249-269

[4] Newmark N.M., Siess C.P., Viest I.M., Test and analysis of composite beam with incomplete interaction, Proceedings of the Society for Experimental Stress Analysis, 1951, 9, 75-92

[5] Girhammar U.A., Gopu V.K.A., Composite beam-columns with interlayer-slip – Exact analysis, ASCE Journal of Structural Engineering,1993, 119(4), 1265-1282

[6] Planinc I., Schnabl S., Saje M., Lopatič J., Čas B., Numerical and experimetnal analysis of timber composite beams with interlayer slip, Engineering Structures, 2009, 30, 2959-2969

[7] Girhammar U.A., Pan D.H., Exact static analysis of partially composite beams and beam-columns, International Journal of Mechanical Sciences, 2007, 49(2), 239-255

[8] Goodman J.R., Popov E.P., Layered beam systems with interlayer slip, Journal of Structures, Division–ASCE,1968, 94(11), 2537-2547

[9] Goodman J.R., Popov E.P., Layered beam systems with interlayer slip, Wood Science, 1969, 1(3), 148-158

[10] Ecsedi I., Dluhi K., A linear model for static and dynamic analysis of nonhomogeneous curved beams, Applied Mathematical Modelling, 2005, 29, 1211-1231

[11] Sokolnikoff I.S., Mathematical Theory of Elasticity, McGraw-Hill, New York, 1956

[12] Thomson F., Goodman, I., Vanderbilt, M., Finite element analysis of layered wood system. Journal of Structural Engineering, 1975, 101(12), 2659-2672

[13] Girhammar, U. A., A simplified analysis method for composite beams with interlayer slip. International Journal of Mechanical Sciences, 2009, 51(7), 515-530.

[14] Ranzi G., Bradford M., Uy B., A direct stiffness analysis of composite beam with partial interaction. Int. Journ. Num. Methods of Engineering, 2004. 61(5), 657-672.

[15] Schnabl S., Saje M., Turk G., Planic I., Locking free two-layer Timoshenko beam element with interlayer slip, 2007, 43(39), 705-714

[16] Saje M., Cas B., planic I., Non-linear finite element analysis of composite planar frames with interlayer slip, Comp. Structures, 2004, 82(23-26), 1901-1912

[17] Liu X., Erkmen R.E Bradford M.A.,Creep and shrinkage composite beams including the effects of partial interaction, Paper 154, Proceedings of the Eleventh International Conference on Computational Structures Technology, B.H.V. Topping, (Editor), Civil-Comp Press, Stirlingshire, Scotland Civil-Comp Press, 2012

[18] Tan E.L., B. Uy B., Nonlinear analysis of composite beams subjected to combined flexure and torsion, Journal of Constructional Steel Research 2011, 67, 790–799

[19] Erkmen R.E, Mark A. Bradford M.A., Nonlinear elastic analysis of composite beams curved in-plan, Engineering Structures, 2009, 31, 1613-1624